AD-A244 692

(2)

OFFICE OF NAVAL RESEARCH

Grant N00014-90-J-1193

TECHNICAL REPORT No. 75

Dynamics of an M-level Atom Interacting with Cavity Fields. III. Nonclassical Behavior of the Initially Squeezed Field

by

Fu-li Li, Xiao-shen Li, D. L. Lin and Thomas F. George

Prepared for publication

in

Physical Review B

Departments of Chemistry and Physics
Washington State University
Pullman, WA 99164-1046

January 1992

UNCLASSIFIED

SECURITY CLASSIFICATION OF THIS PAGE

REPORT DOCUMENTATION PAGE

Form Approved OMB No. 0704-0188

1a. REPORT SECURITY CLASSIFICATION Unclassified	1b. RESTRICTIVE MARKINGS
2a. SECURITY CLASSIFICATION AUTHORITY 2b. DECLASSIFICATION / DOWNGRADING SCHEDULE	3. DISTRIBUTION / AVAILABILITY OF REPORT Approved for public release; distribution unlimited
4. PERFORMING ORGANIZATION REPORT NUMBER(S) WSU/DC/92/TR-75	5. MONITORING ORGANIZATION REPORT NUMBER(S)
6a. NAME OF PERFORMING ORGANIZATION Depts. Chemistry & Physics Washington State University 6b. OFFICE SYMBOL (If applicable)	7a. NAME OF MONITORING ORGANIZATION
6c. ADDRESS (City, State, and ZIP Code) 428 French Administration Building Pullman, WA 99164-1046	7b. ADDRESS (City, State, and ZIP Code) Chemistry Program 800 N. Quincy Street Arlington, Virginia 22217
8a. NAME OF FUNDING / SPONSORING ORGANIZATION Office of Naval Research 8b. OFFICE SYMBOL (If applicable)	9. PROCUREMENT INSTRUMENT IDENTIFICATION NUMBER Grant N00014-90-J-1193
8c. ADDRESS (City, State, and ZIP Code) Chemistry Program 800 N. Quincy Street Arlington, Virginia 22217	10. SOURCE OF FUNDING NUMBERS PROGRAM ELEMENT NO. / PROJECT NO. / TASK NO. / WORK UNIT ACCESSION NO.

11. TITLE (Include Security Classification)
Dynamics of an M-level Atom Interacting with Cavity Fields. III. Nonclassical Behavior of the Initially Squeezed Field

12. PERSONAL AUTHOR(S)
Fu-li Li, Xiao-shen Li, D. L. Lin and Thomas F. George

13a. TYPE OF REPORT	13b. TIME COVERED	14. DATE OF REPORT (Year, Month, Day)	15. PAGE COUNT
	FROM ____ TO ____	January 1992	21

16. SUPPLEMENTARY NOTATION
Prepared for publication in Physical Review B

17. COSATI CODES			18. SUBJECT TERMS (Continue on reverse if necessary and identify by block number)
FIELD	GROUP	SUB-GROUP	CAVITY FIELDS; NONCLASSICAL BEHAVIOR; M-LEVEL ATOM; ANTIBUNCHING; SQUEEZED FIELD; COHERENT EXCITATION

19. ABSTRACT (Continue on reverse if necessary and identify by block number)

The interaction of an M-level atom with a single-mode of cavity field initially in a squeezed state is investigated in this paper. The time evolution of nonclassical characteristics of the field, such as the field squeezing, antibunching and sub-Poisson distribution, are computed and discussed in detail. It is found that the initial coherent excitation strength has crucial influence on how such nonclassical behavior can be maintained in the propagation of squeezed light.

20. DISTRIBUTION / AVAILABILITY OF ABSTRACT ☒ UNCLASSIFIED/UNLIMITED ☒ SAME AS RPT. ☐ DTIC USERS	21. ABSTRACT SECURITY CLASSIFICATION Unclassified
22a. NAME OF RESPONSIBLE INDIVIDUAL Dr. John C. Pazik	22b. TELEPHONE (Include Area Code) (202) 696-4410 22c. OFFICE SYMBOL

DD Form 1473, JUN 86 Previous editions are obsolete.

SECURITY CLASSIFICATION OF THIS PAGE

UNCLASSIFIED

Physical Review B, in press

Dynamics of an M-level Atom Interacting with Cavity Fields. III. Nonclassical Behavior of the Initially Squeezed Field

Fu-li Li
Chinese Center of Advanced Science and Technology (World Laboratory)
P. O. Box 8730, Beijing 100080, and
Department of Modern Physics, Lanzhou University*
Lanzhou 73000, China

Xiao-shen Li and D. L. Lin
Department of Physics and Astronomy
State University of New York at Buffalo
Buffalo, New York 14260

Thomas F. George
Departments of Chemistry and Physics
Washington State University
Pullman, Washington 99164

Abstract

The interaction of an M-level atom with a single-mode of cavity field initially in a squeezed state is investigated in this paper. The time evolution of nonclassical characteristics of the field, such as the field squeezing, antibunching and sub-Poisson distribution, are computed and discussed in detail. It is found that the initial coherent excitation strength has crucial influence on how such nonclassical behavior can be maintained in the propagation of squeezed light.

*Mailing Address

PACS Numbers: 32.80.-t, 42.50.-p, 42.50.Dv

I. Introduction

The interaction of squeezed light[1] with matter has attracted much attention in recent years, especially after the photon squeezed state was experimentally realized.[2-4] The development of micromaser technology and the Rydberg-atom technique has made the Jaynes-Cumming models realistic. As a matter of fact, there have been investigations of a two-level atom with cavity fields initially in various types of squeezed states.[5-12]

When the field is initially in a coherent state, it has been shown[5] that the field may become squeezed via its interaction with the atom. When the field is initially in a squeezed vacuum state, it has also been shown[6] that the field can maintain its squeezing after its interaction with the atom is turned on only if the initial field is very weak or if the initial squeezing is very shallow. Further study shows[7] that the deeper the initial squeezing of the field, the quicker the field loses squeezing during the atom-field interaction.

When the atom interacts with the cavity field which is initially in a coherent squeezed state,[1] the interaction has revealed a number of interesting dynamical properties.[8,9] The coherent squeezed state is characterized by two parameters, α and γ, where α determines the strength of the coherent excitation and γ measures the degree of squeezing. It is interesting to note that photons are not only squeezed in a coherent squeezed state but also exhibit nonclassical behavior as antibunching and subpoisson phenomena.

Recently, a general formalism of the interaction of an M-level atom with initially coherent cavity fields has been developed by the present authors,[13-15] and multiphoton processes involving a realistic Rydberg atom

with nearly equal energy level spacing have been considered. The effect of level number on dynamical properties of both the atom and the field has been discussed in great detail. One of the major findings is that multiphoton cascade processes enhance the nonclassical properties of the cavity field. In this paper, we consider the atom-field interaction in an optical cavity with the field initially in a coherent squeezed state. Nonclassical properties of the field are discussed and their time evolution is investigated.

II. Theory

The general theory of the interaction between an M-level atom and single-mode cavity fields has been formulated in Ref. 13, and only the steps essential for our present discussion are outlined here. We consider an M-level atom as shown schematically in Fig. 1. The total Hamiltonian is given in the rotating-wave approximation by

$$H = \hbar\Omega a^{\dagger}a + \sum_{i=1}^{M} \hbar\omega_i A_i^{\dagger}A_i + \sum_{i=1}^{M} \lambda_i A_{i+1}^{\dagger}A_i a + \text{H.c.}\,, \tag{1}$$

where the operator $a^{\dagger}$ creates a photon of frequency Ω, $A_i^{\dagger}$ creates an atom in its i-th level with energy $\hbar\omega_i$, and λ_i stands for the coupling constant. The state in which the atom is in the i-th level and the number of photons is m is denoted by

$$|i,m\rangle = |i\rangle|m\rangle. \tag{2}$$

If the photon number is n when the atom is in its highest level, an arbitrary state in Hilbert space can be written as

$$|\phi_n> = \sum_{i=1}^{M} C_{i,n+M-i}\ |i,n+M-i>, \tag{3}$$

where the probability amplitude $C_{i,n+M-i'}$ satisfies the stationary-state Schrödinger equation

$$\sum_{i'=1}^{M} [(H_{ii}-E)\delta_{ii'} + H_{ii'}]\ C_{i',n+M-i'} = 0. \tag{4}$$

The matrix elements involved in Eq. (4) are given explicitly by

$$H_{ii} = <i,n+M-i|H|i,n+M-i>$$

$$= (n+M-1)\hbar\Omega+\hbar\omega_1 - \sum_{j=1}^{i-1} \Delta_j \tag{5a}$$

$$H_{ii'} = <i,n+M-i|H|i',n+M-i'>$$

$$= \lambda_{i'}\delta_{i,i'+1}\sqrt{n+M-i'} + \lambda_{i'-1}\delta_{i,i'-1}\sqrt{n+M-i'+1},\ i\neq i', \tag{5b}$$

where we have defined the detuning parameters

$$\Delta_i = \hbar\Omega-\hbar(\omega_{i+1}-\omega_i),\ i=1,2,\ldots.,\ M-1. \tag{5c}$$

The energy eigenfunctions $|\phi_{n\sigma}>$ and their corresponding eigenvalues $E_{n\sigma}$ are found by solving Eq. (4),

$$H\ |\phi_{n\sigma}> = E_{n\sigma}|\phi_{n\sigma}> \tag{6a}$$

$$|\phi_{n\sigma}> = \sum_{i=1}^{M} C^{\sigma}_{i,n+M-1}|i,n+M-i>, \tag{6b}$$

where σ is introduced just to label the eigenstates.

In the representation spanned by the energy eigenstates $|\phi_{n\sigma}>$, the density matrix elements take the form

$$\rho_{n\sigma,n'\sigma'}(t) = \rho_{n\sigma,n'\sigma'}(0)\ \exp[-\frac{i}{\hbar}(E_{n\sigma}-E_{n'\sigma'})t] \tag{7a}$$

with the initial matrix elements

$$\rho_{n\sigma,n'\sigma'}(0) = \rho_{nn'}(C^{-1})^{M}_{\sigma,n+M-\sigma}\ (C^{-1})^{M}_{\sigma',n'+M-\sigma'}. \tag{7b}$$

Here, $\rho_{nn'}$ are the density matrix elements of the initial field in the Fock representation, and C^{-1} is the inverse of the matrix defined in Eq. (3). For any arbitrary function F of the field operators or any function A of the atomic operators, the mean values are calculated according to the following expressions:

$$<F> = Tr(\rho F) = \sum_{n\sigma} <n\sigma|\rho F|n\sigma>$$

$$= \sum_{n,n'=0}^{\infty} \sum_{\sigma,\sigma'=1}^{M} \sum_{i=1}^{\infty} C^{\sigma}_{i,n+M-i}\ C^{\sigma'}_{i',n'+M-i} <n'+M-i|F|n+M-i> \rho_{n\sigma,n'\sigma'}(t) \tag{8}$$

$$<A> = Tr(\rho F) = \sum_{n\sigma} <n\sigma|A|n\sigma>$$

$$= \sum_{n,n'=0}^{\infty} \sum_{\sigma,\sigma'=1}^{M} \sum_{i=1}^{M} C^{\sigma}_{i,n+M-i}\ C^{\sigma'}_{n'-n+i,n+M-i} <n'-n+i|A|i> \rho_{n\sigma,n'\sigma'}(t). \tag{9}$$

III. Evolution of the Field Squeezing

We assume that the cavity field is initially in a coherent squeezed state[1]

$$|\alpha,\gamma\rangle = e^{\alpha a^\dagger - \alpha^* a}\, e^{\gamma(a^2 - a^{\dagger 2})/2}|0\rangle = \sum_{n=0}^{\infty} C_n|n\rangle, \tag{10}$$

where

$$C_n = (n!\mu)^{-½} \left(\frac{v}{2\mu}\right)^{n/2} H_n(\beta/\sqrt{2\mu v})\ \exp(-½|\beta|^2 + \frac{v^*}{2\mu}\beta^2) \tag{11}$$

with H_n the nth-order Hermite polynomial and

$$\beta = \alpha\mu + \alpha^* v. \tag{12}$$

$$\mu = \cosh\gamma,\ v = \sinh\gamma. \tag{13}$$

Thus, the initial density matrix elements of the cavity field are

$$\rho_{nn'} = C_n^* C_{n'}. \tag{14}$$

In our numerical work throughout this paper, we have taken $\hbar = 1$. We have also assumed for simplicity the same coupling constant $\lambda_i = \lambda$ for any i and zero detuning for any transition. The unit of time is $1/\lambda$. Since we are only interested in the effect of the coherent excitation strength $|\alpha|^2$ on the dynamical behavior of the atom and on the statistical properties of the field, we have assumed a real α, namely, the squeezing to be in the direction of the coherent excitation.

Consider two Hermitian time-dependent quadrature operators of the field

$$a_1 = \frac{1}{2}(ae^{i\Omega t} + a^\dagger e^{-i\Omega t}) \tag{15a}$$

$$a_2 = \frac{1}{2i}(ae^{i\Omega t} - a^\dagger e^{-i\Omega t}). \tag{15b}$$

The field is said to be in the squeezed state if either of the operators satisfies $\langle(\Delta a_i)^2 = \langle a_i^2\rangle - \langle a_i\rangle^2 < 1/4.$[14] The variances for a_1 and a_2 of the initial field are found from Eq. (10) to be

$$\langle(\Delta a_1)^2\rangle = ¼e^{-2\gamma} \tag{16a}$$

$$<(\Delta a_2)^2> = \frac{1}{4}e^{2\gamma}, \tag{16b}$$

respectively. It is obvious that the quantum fluctuation of a_1 initially is smaller than the quantum limit $\frac{1}{4}$, and that the degree of the field squeezing is completely determined by the parameter γ and is independent of the coherent strength $|\alpha|^2$. For the time evolution of the squeezing, however, the coherent strength plays a very important role as we shall see later.

In micromaser experiments, the atom stays in the cavity only for a short time,[16,17] and the excited levels are short-lived. The study of the short-time evolution of the field squeezing is therefore of particular interest for the experimental preparation of squeezed states in the micromaser cavity. In Figs. 2 - 4 we plot the variance $<(\Delta a_1)^2>$. For given M and λ, the variance becomes an oscillating function of time, with the oscillation frequency increasing with $|\alpha|^2$. It is also clearly seen that the field remains squeezed much longer as the coherent strength increases. When α and γ are fixed, the calculation shows that increasing the level number M decreases the oscillating frequency.

The mean photon number $<n>$ in the initial field (10) is

$$<n> = <a^\dagger a> = |\alpha|^2 + \sinh^2\gamma. \tag{17}$$

For a fixed initial squeezing, Eq. (17) implies that increasing coherent strength means increasing the intensity of the initial field. Hence, our results indicate that for fixed $<n>$ the field can maintain its squeezing for a long time during its interaction with the atom only if the coherent part and the squeezing part are properly adjusted. In general, the atom-field interaction helps sustain the field squeezing for sufficiently large

$|\alpha|^2$, and the field is further squeezed if γ is small enough, i.e., a shallow squeezed field initially.

IV. Antibunching and Sub-Poisson Distribution

It is well known that photon statistical properties depend on the normalized intensity correlation function of the field defined by

$$g^{(2)}(t) = <[a^\dagger(t)]^2[a(t)]^2>/<a^\dagger(t)a(t)>. \tag{18}$$

when $g^{(2)} = 1$, the field is in coherent state and the photon distribution is Poissonian. When $g^{(2)} < 1$, the field exhibits photon antibunching and a sub-Poisson distribution, and when $g^{(2)} > 1$, the field exhibits photon bunching and a super-Poisson distribution. For the coherent squeezed state (10), we find

$$g^{(2)}(0) = 1 - \frac{2\alpha^2(1-e^{-2\gamma}) + \cosh 2\gamma(1-\cosh 2\gamma)}{2(\alpha^2 + \sinh^2\gamma)^2}. \tag{19}$$

Evidently, initial antibunching is possible only if the parameters α and γ are sufficiently small. We have computed $g^{(2)}(t)$ for $\alpha = 1$ and $\gamma = 0.2$, for which $g^{(2)}(0) = 0.74$. The results are plotted in Fig. 5 for M = 2, 6 and 10. It is observed that for M = 2, $g^{(2)}(t)$ oscillates around its initial value for long times. Furthermore, the value of the correlation function remains less than unity except for a few isolated instants.

For many-level atoms, the calculation shows that the antibunching effect is greatly weakened after the atom-field interaction takes place. For M = 10, photon antibunching quickly disappears and $g^{(2)}$ oscillates most of the time above unity. We have also found in our numerical study that the oscillation amplitude reduces dramatically as the initial coherent strength increases. For a given squeezing parameter, it is always possible to

achieve photon antibunching for a long time by increasing the initial coherent strength. Of course, the antibunching may be very weak when $|\alpha|^2$ becomes too large.

The deviation of the photon number probability from the Poisson distribution can be directly measured by the Q-parameter related to $g^{(2)}$ by

$$Q(t) = \langle a^\dagger(t)a(t)\rangle[g^{(2)}(t)-1] \tag{20}$$

for a single-mode field. Thus, antibunching implies a sub-Poisson distribution and vice versa for the case of single-mode fields. It is, however, important to emphasize that a sharp sub-Poisson distribution does not necessarily imply strong antibunching. In fact, as can be seen from Eq. (20), a large mean photon number can produce a near-photon-number eigenstate for which Q = -1 even though $g^{(2)}$ is just slightly below 1.

For the coherent squeezed state (10), we find

$$Q = \frac{|\alpha|^2 e^{-2\gamma} + \frac{1}{2}\sinh^2 2\gamma}{|\alpha|^2 + \sinh^2\gamma} - 1. \tag{21}$$

It is easily seen from Eq. (21) that for a given squeezing paramter γ, one can always achieve a sub-Poisson distribution by increasing $|\alpha|^2$. The Q-values for fixed $|\alpha|^2$ are plotted as functions of γ in Fig. 6. We notice that the Q-value becomes smaller as the coherent excitation $|\alpha|^2$ increases if the squeezing parameter γ is kept constant. For every given $|\alpha|^2$, there exists a γ-value for which Q is minimum, which decreases and approaches the limit -1 as $|\alpha|^2$ increases.

The time evolution of the Q-value for atoms with different level numbers is shown in Fig. 7. We take $|\alpha|^2 = 25$ and $\gamma = 0.8$, whereby the initial Q-value is -0.69 according to Fig. 6. For the whole time range that we have calculated, Q remains negative or the photon probability

remains a sub-Poisson distribution. This is true as long as the initial Q-value is sufficiently small. The collapse and revival appear clearly, especially for small M.

In coherent squeezed states of the field, the photon exhibits nonclassical behavior as antibunching and a sub-Poisson distribution. When the coherent strength is weak, the antibunching property is more dramatic, and when the coherent strength is strong, the sub-Poisson distribution becomes more distinct. For sufficiently small M such nonclassical properties can be maintained for a long time during the atom-field interaction process. Thus, for an initially squeezed photon state, cascade multiphoton processes in the atom-field interaction tend to screen out nonclassical properties of the field, in contrast to the case for an initially coherent state.[14,15] In conclusion, this study helps us choose a suitable component of coherent excitation part in the squeezed light so that nonclassical properties can be sustained during its propagation.

Acknowledgments

This research was supported in part by the National Science Foundation under Grant CHE-9016789 and by the Office of Naval Research.

References

1. H. P. Yuen, *Phys. Rev. A* 13, 2226 (1976).
2. R. E. Slusher, L. W. Hollberg, B. Yurk, J. C. Mertz and J. F. Valley, *Phys. Rev. Lett.* 55, 2409 (1985); 56, 788 (1986).
3. R. M. Shelby, M. D. Levenson, S. H. Perlmutter, R. V. DeVoe and D. F. Walls, *Phys. Rev. Lett.* 57, 691 (1986).
4. L. A. Wu, H. J. Kimble, J. L. Hall and H. Wu, *Phys. Rev. Lett.* 57, 2520 (1986).
5. P. Meystre and M. S. Zubairy, *Phys. Lett. A* **89**, 390 (1982).
6. J. Gea-Banacloche, R. R. Schlicher and M. S. Zubairy, *Phys. Rev. A* 38, 3514 (1988).
7. V. Buzk, *Phys. Lett. A* 139, 231 (1989); *Phys. Rev. A* **39**, 3196 (1989).
8. M. V. Satyanarayana, P. Rice, R. Vyas and H. J. Carmichael, *J. Opt. Soc. Am. B* **6**, 228 (1989).
9. G. J. Milburn, *Optica Acta* 31, 671 (1984).
10. Shi-Yao Zhu and M. O. Scully, *Phys. Lett. A* 130, 101 (1988); 133, 95 (1988).
11. C. C. Gerry, *Phys. Rev. A* 37, 2683 (1988).
12. Lin-Sheng He, *J. Opt. Soc. Am. B* **6**, 1915 (1989).
13. Fu-Li Li, D. L. Lin, T. F. George and X. S. Li, *Phys. Rev. A* 40, 1394 (1989).
14. Fu-li Li, X. S. Li, D. L. Lin and T. F. George, *J. Phys. B* 22, 2977 (1989).
15. Fu-li Li, X. S. Li, D. L. Lin and T. F. George, *Phys. Rev. A* 40, 5129 (1989).

16. D. Meschede, H. Walther and G. Muller, *Phys. Rev. Lett.* 54, 551 (1985).

17. G. Rempe, H. Walther and M. Klein, *Phys. Rev. Lett.* **58**, 353 (1987).

Figure Captions

1. Schematic diagram of the atomic levels.
2. Time evolution of the variance $<(\Delta a_1)^2>$ for M = 2. The solid line is for γ = 0.2, dashed line for γ = 0.6 and dot-dashed line for γ = 1.0. (a) α = 1.0, (b) α = 3.0, (c) α = 5.0.
3. Same as Fig. 2 except M = 6.
4. Same as Fig. 2 except M = 10.
5. Time volution of $g^{(2)}(t)$ for the squeezed field with α = 1.0 and γ = 0.2. (a) M = 2, (b) M = 6, (c) M = 10.
6. Initial correlation $g^{(2)}$ of the squeezed field as a function of the squeezing parameter γ. The solid line is for $|\alpha|^2$ = 25, dot-dashed line for $|\alpha|^2$ = 49.
7. Time evolution of the Q-value with $|\alpha|^2$ = 25 and γ = 0.8. (a) M = 2, (b) M = 6, (c) M = 10.

Li et al
Fig. 1.

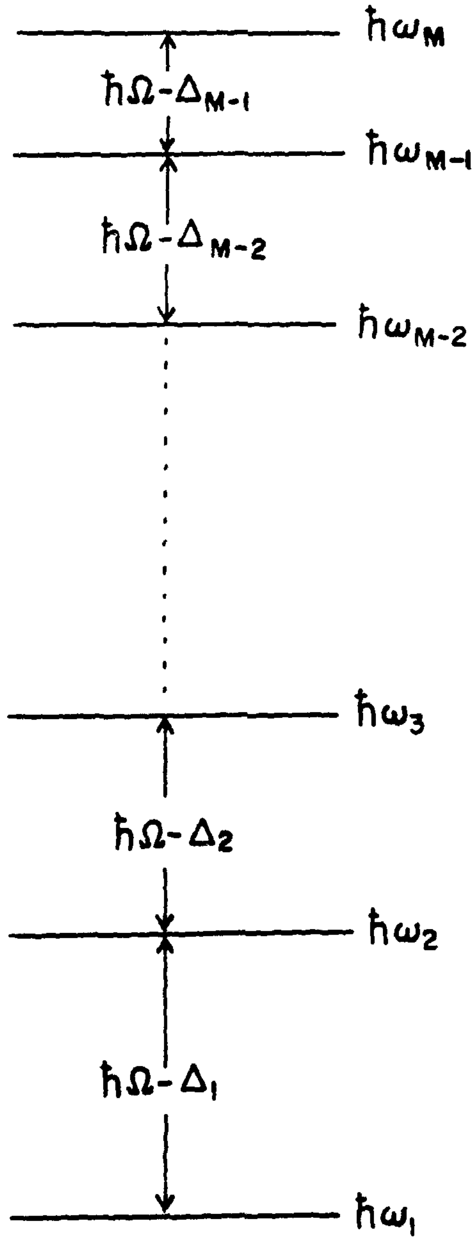

$\hbar\omega_M$
$\hbar\Omega-\Delta_{M-1}$
$\hbar\omega_{M-1}$
$\hbar\Omega-\Delta_{M-2}$
$\hbar\omega_{M-2}$
$\hbar\omega_3$
$\hbar\Omega-\Delta_2$
$\hbar\omega_2$
$\hbar\Omega-\Delta_1$
$\hbar\omega_1$

Li et al

Fig. 2

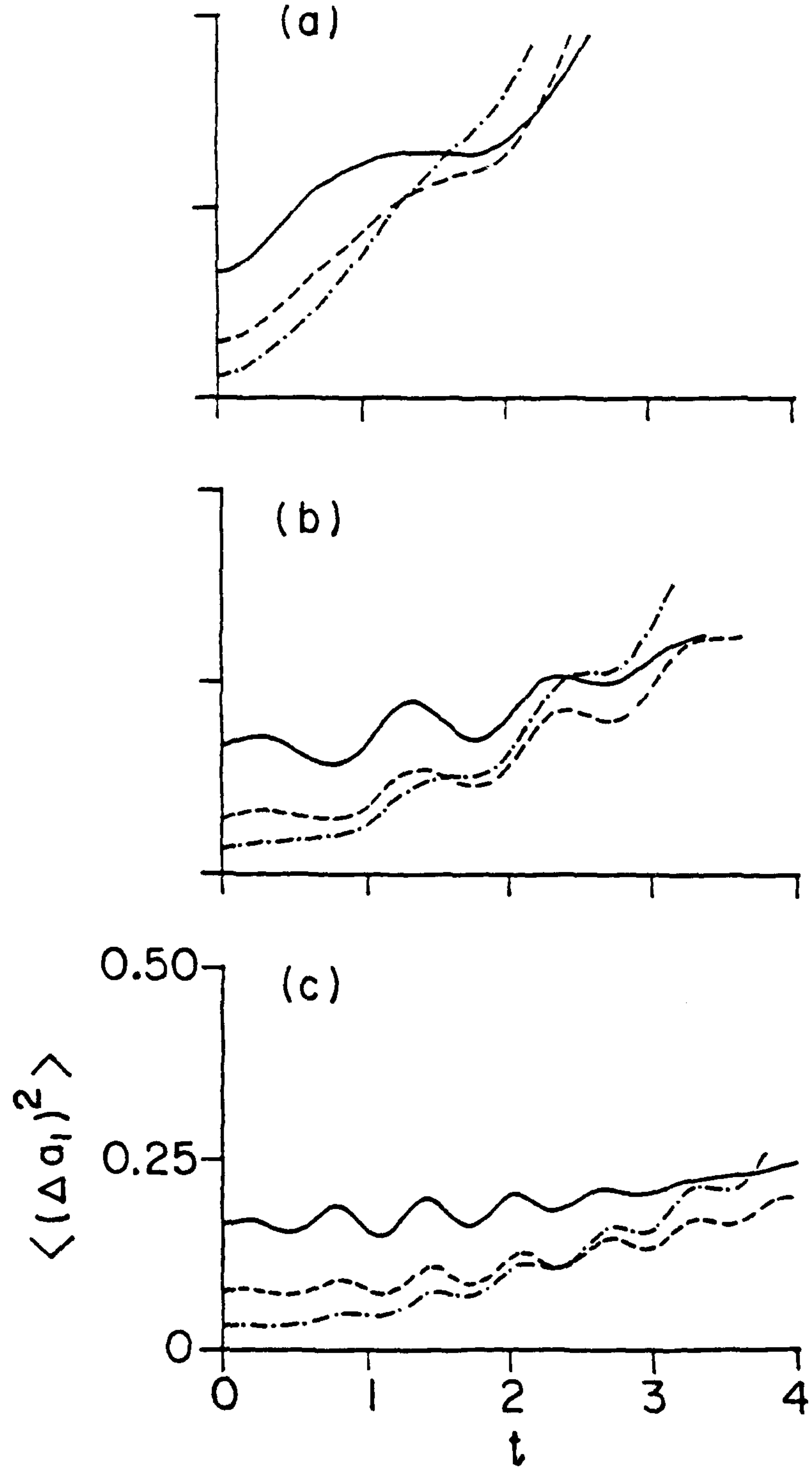

Li et al
Fig. 3

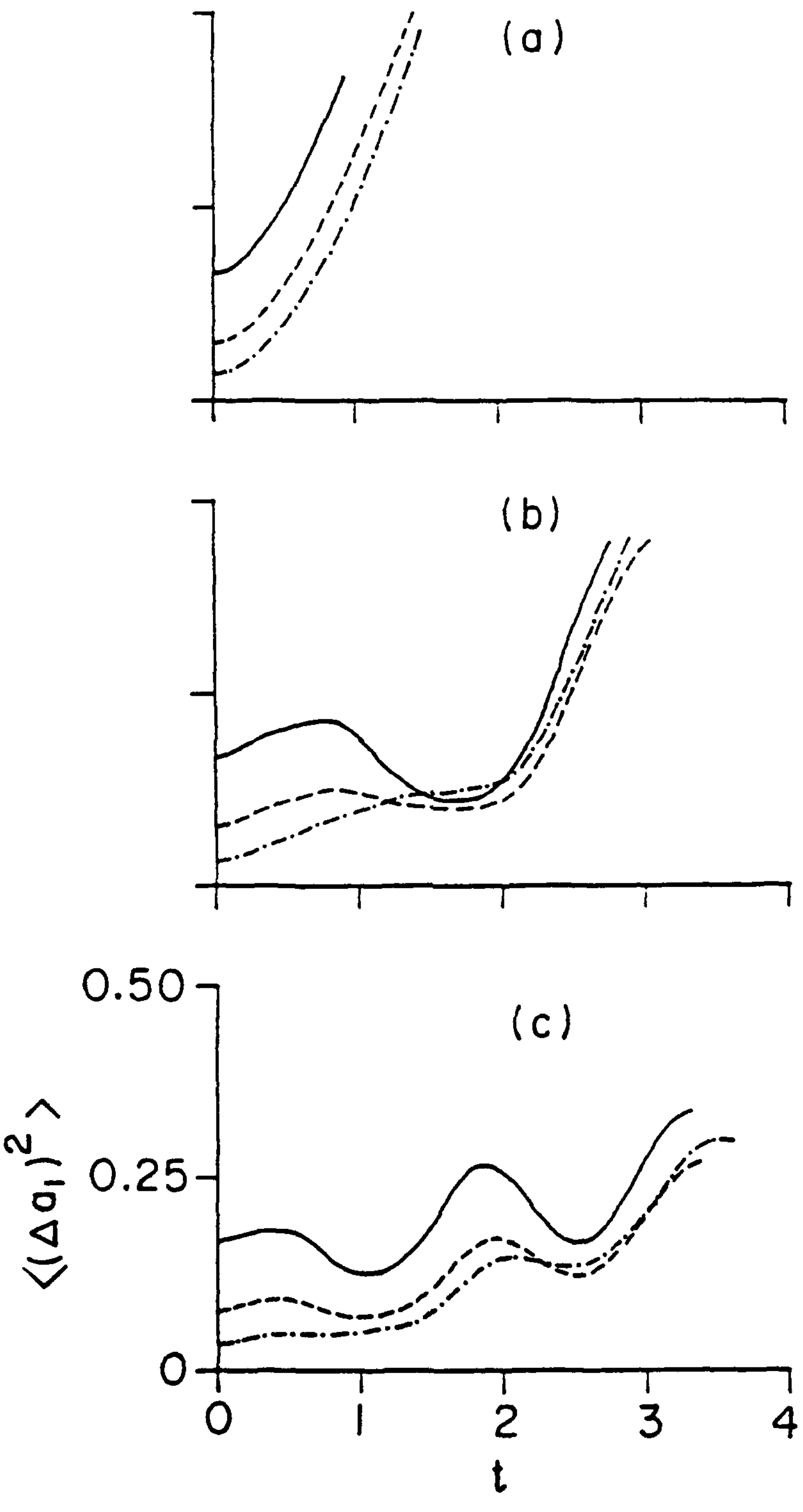

Li et al
Fig. 4

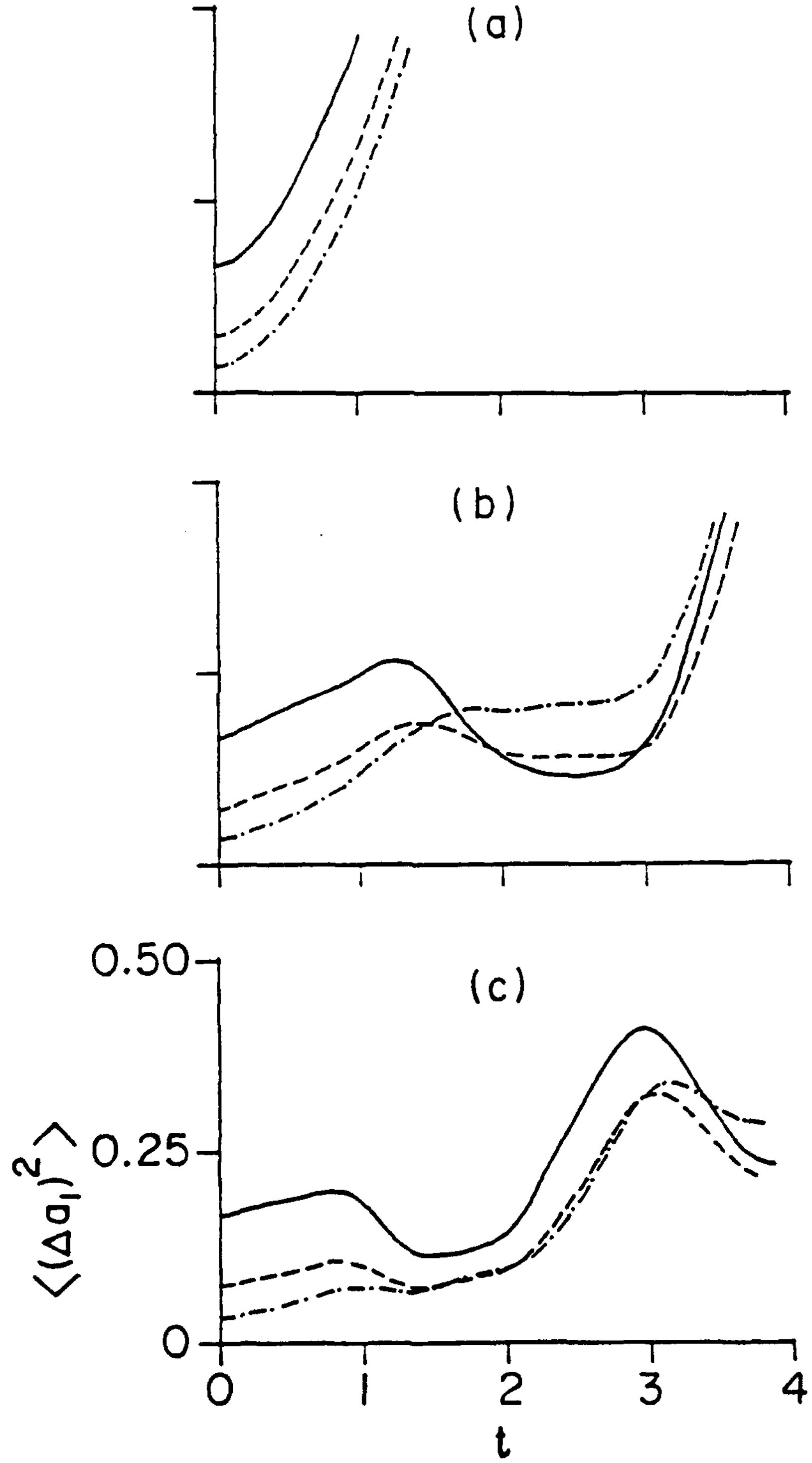

Li et al

Fig. 5

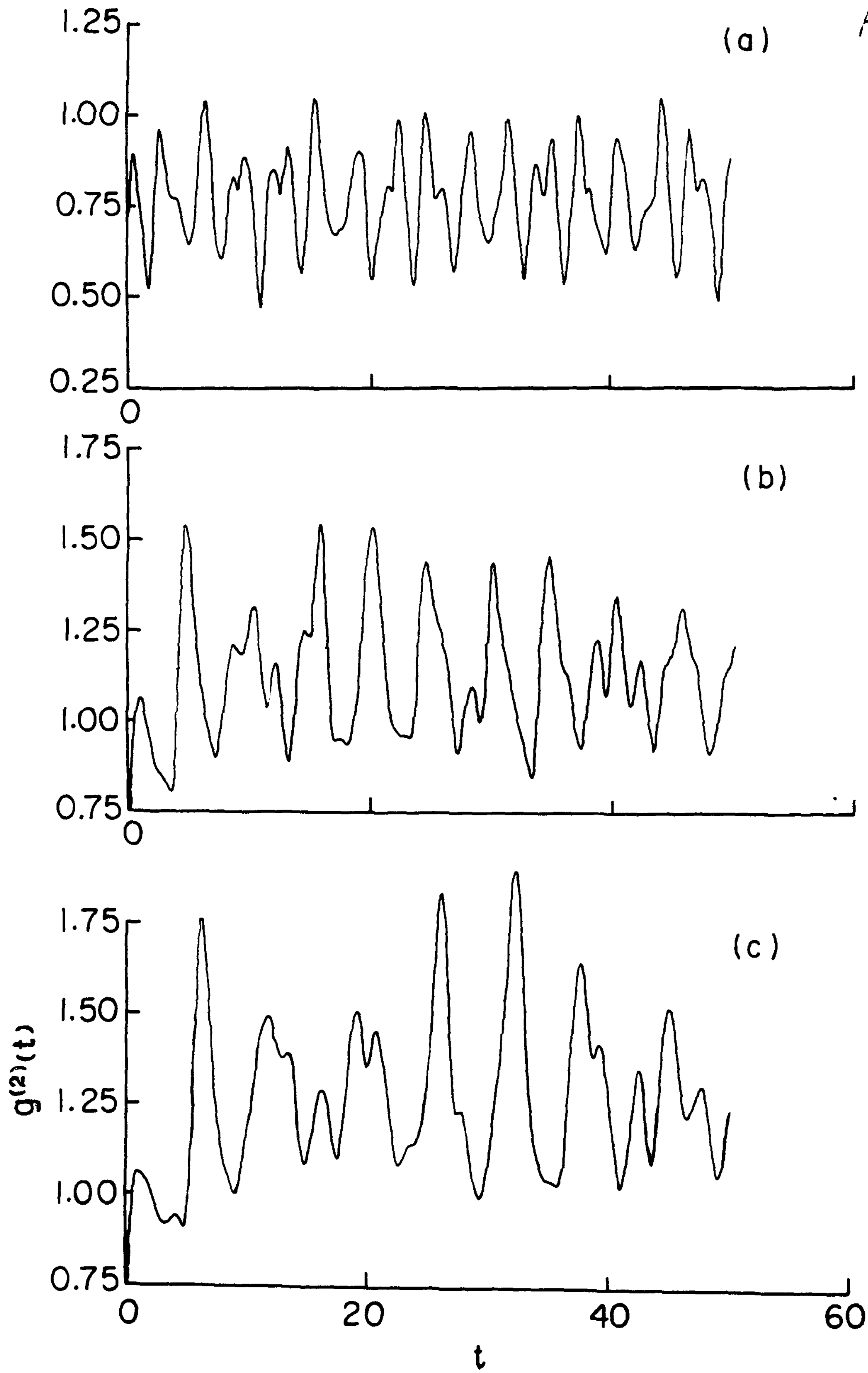
(a)
1.25
1.00
0.75
0.50
0.25
0
(b)
1.75
1.50
1.25
1.00
0.75
0
(c)
$g^{(2)}(t)$
1.75
1.50
1.25
1.00
0.75
0
20
40
60
t

Li et al
Fig. 6

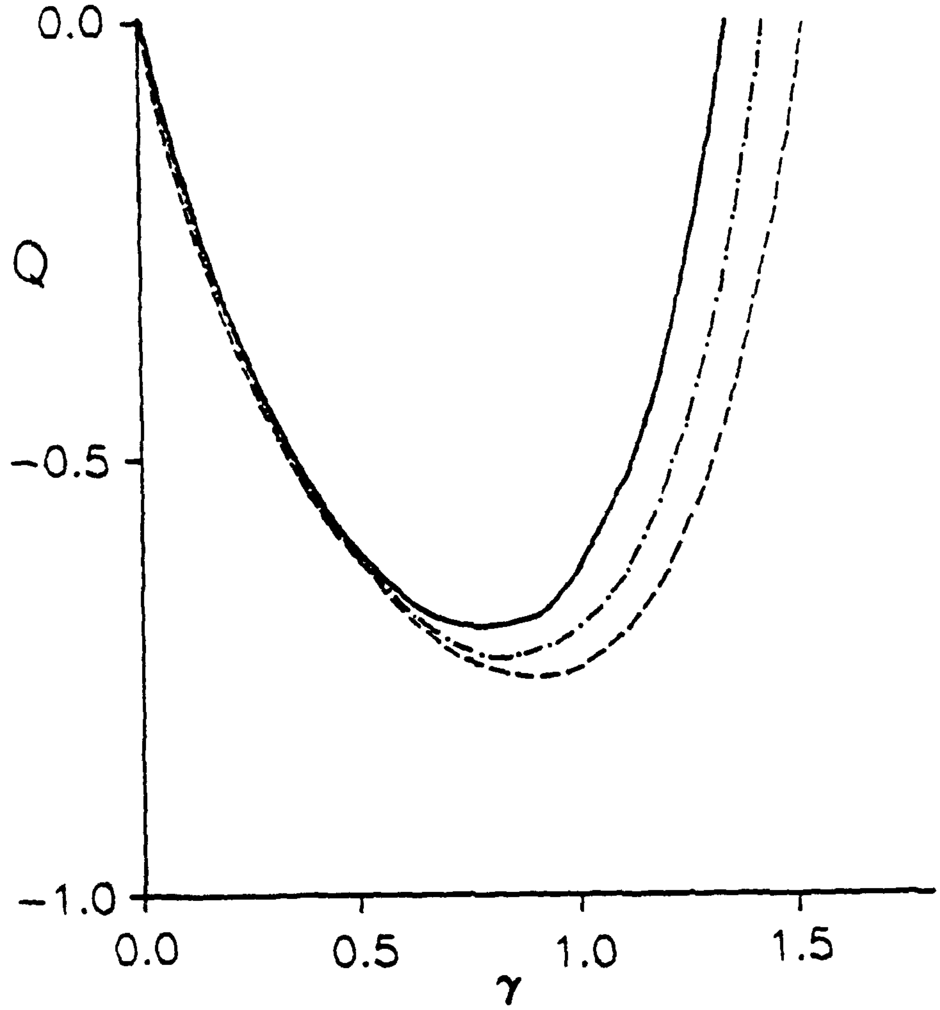

Li et al
Fig. 7